

## Article

# A Comprehensive Framework for Evaluating Bridge Resilience: Safety, Social, Environmental, and Economic Perspectives

Yanjie Liu <sup>1</sup> and Cheng Xiang <sup>2,\*</sup><sup>1</sup> Department of Bridge Engineering, Tongji University, Shanghai 200092, China; lyj1995@tongji.edu.cn<sup>2</sup> College of Civil Engineering, Fuzhou University, Fuzhou 350116, China

\* Correspondence: chengxiang@fzu.edu.cn

**Abstract:** Bridges are critical components of transportation systems and are susceptible to various natural and man-made disasters throughout their lifecycle. With the rapid development of the transportation industry, the frequency of vehicle-induced disasters has been steadily increasing. These incidents not only result in structural damage to bridges but also have the potential to cause traffic interruptions, weaken social service functions, and impose significant economic losses. In recent years, research on resilience has become a new focus in civil engineering disaster prevention and mitigation. This study proposes a concept of generalized bridge resilience and presents an evaluation framework for cable-stayed bridges under disasters. The framework includes a resilience evaluation indicator system from multiple dimensions, including safety, society, environment, and economy, which facilitates the dynamic and comprehensive control of bridge resilience throughout its entire lifecycle with the ultimate goals of enhancing structural safety and economic efficiency while promoting the development of environmentally friendly structural ecosystems. Furthermore, considering the influence of recovery speed, the study evaluates various repair strategies through resilience assessment, revealing the applicable environments and conditions for different repair strategies. This methodology offers significant implications for enhancing the safety, efficiency, and environmental sustainability of infrastructure systems, providing valuable guidance for future research in this field.



**Citation:** Liu, Y.; Xiang, C. A Comprehensive Framework for Evaluating Bridge Resilience: Safety, Social, Environmental, and Economic Perspectives. *Sustainability* **2024**, *16*, 1135. <https://doi.org/10.3390/su16031135>

Academic Editors: Xander Wang and Aminur Shah

Received: 2 January 2024

Revised: 26 January 2024

Accepted: 27 January 2024

Published: 29 January 2024



**Copyright:** © 2024 by the authors. Licensee MDPI, Basel, Switzerland. This article is an open access article distributed under the terms and conditions of the Creative Commons Attribution (CC BY) license (<https://creativecommons.org/licenses/by/4.0/>).

**Keywords:** resilience; evaluation framework; disaster; functionality

## 1. Introduction

Bridges, serving as critical channels for human socioeconomic activities, face vulnerabilities to a wide range of hazards. Natural disasters or technologically-induced extreme events (such as fires, explosions, or even deliberate acts of terrorism) can pose significant risks to the structural integrity of bridges. Therefore, the development of theories and technologies focused on preventing and mitigating bridge disasters has become an urgent priority.

In recent years, there has been notable emphasis on the concept of resilience and an increased interest in its practical implementation. The concept of resilience was first introduced by Holling [1] in the study of ecosystems. He defined resilience as the extent to which a system can withstand external disturbances without undergoing significant changes. In 1981, Timmerman [2] put forth the most widely accepted definition of resilience to date: “Resilience is the ability of human communities to withstand external shocks or perturbations to their infrastructure and to recover from such perturbations”. Over the preceding years, a number of comprehensive definitions of resilience, along with frameworks outlining its practical implementation, have been put forward. Bruneau et al. [3] presented a framework to define and quantitatively measure the seismic resilience of communities. Rose [4] introduced major conceptual, operational, and policy analysis advances in evaluating individual and regional economic resilience to disasters. Miles and

Chang [5] set out a conceptual model specifying linkages between sectors, domains, scales, and processes in community recovery from earthquakes and other disasters.

Across various research domains, the definitions of resilience share common origins and characteristics. However, they may differ in terms of the targeted systems and emphasized aspects. The resilience of engineering structures is often interconnected with robustness and structural restoration. The former ensures the reliability of structures under extreme disaster conditions, while post-disaster functionality recovery capability guarantees the speed at which the system can return to use. More specifically, within the realm of civil engineering, resilience is primarily associated with mitigating losses resulting from disasters and effectively managing them. Coppola [6] provided a comprehensive overview of the processes and special issues involved in the management of large-scale natural and technological disasters. Deptuła et al. [7] proposed a prototype risk assessment method based on the assumptions of the SWOT and TOWS analysis and the multi-criteria technical innovation risk assessment method. Frangopol and Bocchini [8] summarized techniques for transportation network analysis and performance assessment. Cimellaro et al. [9] proposed a framework for the evaluation of health care facilities subjected to earthquakes. Chang and Shinozuka [10] proposed resilience measures that relate expected losses in future disasters to a community's seismic performance objectives and demonstrated these measures in a case study of the Memphis, Tennessee, water delivery system.

Currently, there is a wealth of research outcomes concerning urban resilience. The research scope goes beyond the initial focus on natural ecosystems, leaving its mark in numerous disciplinary domains. Martin and Sunley [11] studied the meaning and explanation of regional economic resilience and how it links to patterns of long-run regional growth. Zeng et al. [12] identified key indicators of urban resilience under three major components: adaptive capacity, absorptive capacity, and transformative capacity. Zhou and Chen [13] developed a resilience metric to measure the performance of airport resilience under various severe weather conditions. Wei et al. [14] approached resilience assessment by measuring and comparing the performance of elements or a system before and after a disruptive event.

Given their pivotal status as critical transportation nodes, bridges hold paramount significance within the transportation network. However, there is still a scarcity of research on the resilience of bridge structures. Current investigations are primarily centered within the seismic resilience domain with a prevailing emphasis on either transportation networks or structural resilience. Venkittaraman [15] analyzed the seismic resilience of a reinforced concrete bridge. Alipour and Shafei [16] studied the seismic resilience of highway bridge networks exposed to deterioration processes. Giouvanidis and Dong [17] investigated the seismic performance of single-column bridges, including seismic losses, post-earthquake functionality and resilience. Shen et al. [18] proposed three strategies for enhancing the seismic-damage resistance of PRC piers. Khan et al. [19] used the Dempster–Shafer rule of combination to assess the seismic resilience of a highway bridge by proposing a bridge resilience index. In addition to the traditional safety assessment of bridges, there is a deficiency in multi-dimensional indicators for a comprehensive resilience evaluation. The resilience of bridges under disasters involves multiple disciplines, including disaster studies, engineering, sociology, and economics. Currently, a universally accepted resilience assessment method is lacking due to its complexity.

Drawing upon the foundational tenets of lifecycle assessment, risk analysis, cost evaluation, and resilience theory, this paper presents an evaluative approach to quantifying the diverse dimensions of bridge resilience. The methodology involves a case study assessing bridge resilience under vehicle-induced disasters, considering the progressive deterioration of structural performance due to environmental effects. Additionally, this study outlines the selection of optimal repair strategies based on the resilience evaluation outcomes.

## 2. Methodology for Assessing Bridge Resilience

### 2.1. Analytical Definitions of Resilience

The definition of resilience is founded on a clear understanding of functionality. Different structures or systems have varying interpretations of functional significance, and within a single system, diverse indicators exist that define its functionality [20,21].

#### 2.1.1. Functionality Recovery Models of Bridges

The functionality of a bridge under the influence of disasters can be quantified through various damage states. In this study, the bridge's traffic-carrying capacity is utilized to define its functionality in the range of [0, 1]. When the structure is undamaged, the value is 1. Conversely, when the structure is completely damaged, the value is 0. By categorizing the bridge's damage states into five distinct levels, the expected functionality value of the bridge can be computed as the sum of the product of the functionality value corresponding to each damage state and the probability of being in that state. The quantitative calculation formula [21] for bridge functionality is represented by Equation (1).

$$Functionality = \sum_{i=1}^5 FR_i \times P_{S=DS_i|IM} \quad (1)$$

where  $FR_i$  represents the functionality value corresponding to the damage state  $i$ ;  $P_{S=DS_i|IM}$  represents the probability that the bridge is in the damage state  $i$  under a specific intensity of disaster  $IM$ .

A typical functionality changes process after a disaster is given in Figure 1. Prior to the occurrence of disasters, it is important to consider the potential functionality degradation caused by environmental factors and the cumulative damage caused by previous loads. In this regard, functionality may have already decreased (as depicted in Figure 1, where it is assumed that the functionality of the bridge has decreased to 80% of its original capacity). To begin with, assume that a disaster occurs at point A, causing a certain level of damage to the structure such that its functionality degrades to point B. Subsequently, the BC stage represents the post-disaster suspension period, during which the extent of damage to the structure is assessed over a time range  $\delta_i$ . This assessment involves planning for later restoration work, conducting site cleanup, and keeping the functionality unchanged until time  $t_i$ . During the CD stage, the structural restoration process unfolds, which is characterized by a diverse range of curves due to the variability and complexity introduced by different disaster types, scenarios, repair methods, and available resources. Eventually, at the restoration endpoint  $t_r$ , the functionality returns to a specific target value, signifying the formal completion of the repair efforts. By connecting the post-disaster point B with the restoration endpoint D, a straight-line BD is obtained. The slope of this line is defined as a parameter to quantify the rate at which functionality is restored, which is commonly known as the recovery speed.

The post-disaster functionality restoration process is filled with various uncertainties and can be regarded as a function of a series of random variables. In line with the definition of resilience, it can be concluded that the resilience of a bridge depends on both its resistance capacity against disasters and the subsequent functionality restoration process [5]. Therefore, establishing a well-defined restoration model is crucial for conducting the research on bridge resilience. Due to the absence of precise engineering data, it is not feasible to accurately calculate the process of structural restoration. However, an analytical approach using a finite number of random variables can be employed to estimate the restoration process. Currently, researchers have proposed various functionality recovery models to depict the process of restoring functionality following the occurrence of disasters [20,22–24]. These models encompass linear, exponential, trigonometric, Gaussian cumulative distribution, step-wise, six-parameter models, etc. Among them, the six-parameter model [24] is employed to simulate the functionality restoration process in this study, which can depict

various potential types of functionality recovery for different structural systems by altering the values of the relevant parameters.

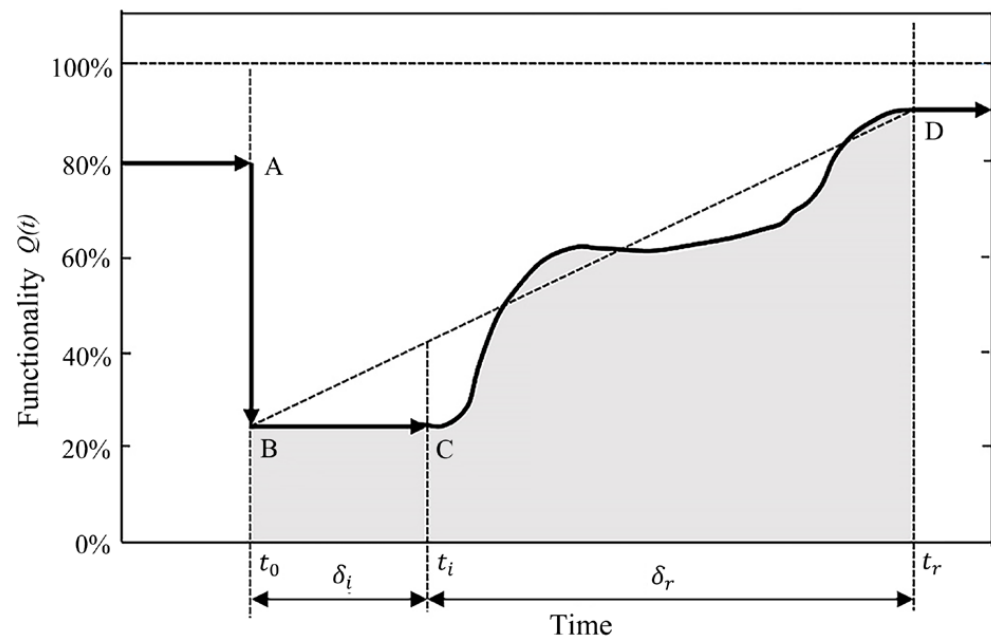


**Figure 1.** Functionality curve of a bridge under the influence of disasters.

As the name implies, the determination of this functionality restoration model involves six parameters: the remaining functionality of the structure  $Q_r$ , the suspension period  $\delta_i$ , the duration of restoration  $\delta_r$ , the target functionality of the structure  $Q_t$ , and the shape parameters  $A$  and  $s$  of the restoration curve. The computational formula for this model [24] is as shown in Equation (2).

$$Q(t > t_0) = Q_r + H[t - t_0 - \delta_i] \cdot f(t - \delta_i) \quad (2)$$

where  $H[x]$  denotes the Heaviside unit step function, and  $f(x)$  is derived from a series of transformations of a sinusoidal function.

The impact of different parameter values on the functionality restoration curve is illustrated in Figure 2. It can be clearly observed that various parameter values exert a noteworthy influence on the construction of the functionality recovery curve, which in turn is intricately linked to the structural environment and the resources available for repair. Consequently, it is imperative to undertake a comprehensive analysis, drawing upon expert surveys, post-disaster structural repair cases, engineering expertise, and on-site conditions to derive estimated values and statistical distributions for these parameters.

### 2.1.2. Quantitative Calculation of Resilience

For a defined functionality recovery profile  $Q(t)$ , Bocchini and Frangopol [21] introduced a quantitative formula for resilience, as shown in Equation (3).

$$R_0 = \int_{t_0}^{t_0+t_h} Q(t) dt \quad (3)$$

where  $t_0$  represents the moment when the extreme event occurs, and  $t_h$  represents the investigated time horizon.

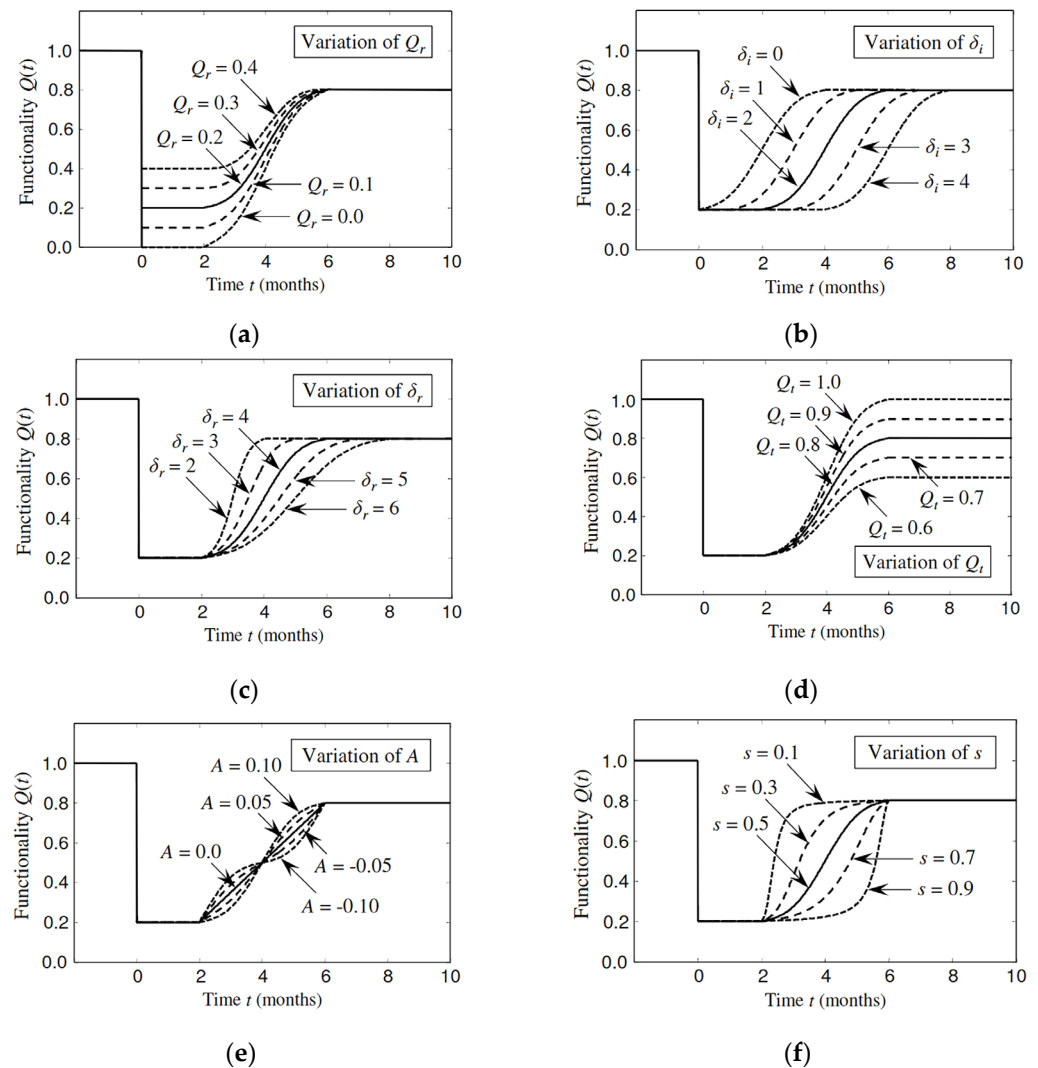


**Figure 2.** Effect of the six parameters on the shape of the functionality recovery model [24]. (a) Variation of  $Q_r$ ; (b) variation of  $\delta_i$ ; (c) variation of  $\delta_r$ ; (d) variation of  $Q_t$ ; (e) variation of  $A$ ; (f) variation of  $s$ .

The definition of resilience presented in Equation (3) proves valuable for comparing, ranking, and optimizing diverse disaster management strategies. However, expressing resilience values in units of time may pose challenges in terms of interpretation and effective communication to decision-makers. To address this issue, a formula that removes the effect of time was proposed [9,25], as illustrated in Equation (4).

$$R = \frac{\int_{t_0}^{t_0+t_h} Q(t) dt}{t_h} \quad (4)$$

Equation (4) provides a scalar in the range of [0, 1] that comprehensively reflects the resilience of the structure, which is currently one of the most widely used formulas for resilience calculation. In this study, this equation was also adopted to quantify the resilience of bridge structures.

In reality, bridges are subjected to significant environmental influences throughout their entire lifespan, especially due to the limited protective measures and their direct exposure to the environment. Taking chloride ion intrusion as an example, it induces concrete carbonation and steel corrosion, causing the functionality of the bridge to decrease and consequently affecting the structural resilience. A schematic diagram illustrating the impact of varying degrees of environmental effects on the functionality and structural resilience of bridges is presented in Figure 3.

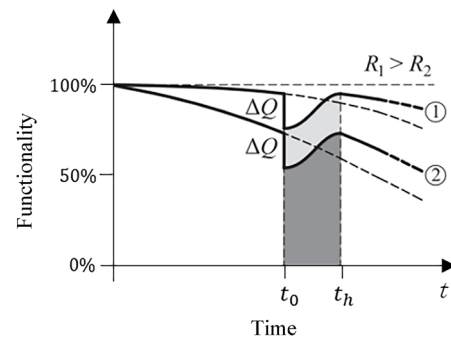


**Figure 3.** The impact of environmental effects on the functionality of bridges.

### 2.2. Bridge Resilience Assessment Method and Process

Current research on assessing bridge resilience is primarily focused on the robustness of bridge structures, estimating bridge structural resilience using relevant analytical formulas. This kind of approach concentrates on the structural safety of bridges while neglecting the potential social, environmental, and economic impacts throughout the entire disaster process, which represents a simplistic and narrow understanding of resilience. Given the limitations of existing research, a generalized bridge resilience concept is proposed, and a methodology for assessing bridge resilience is established in this section. The process for evaluating the generalized resilience of bridges under disasters entails the following steps, as shown in Figure 4.

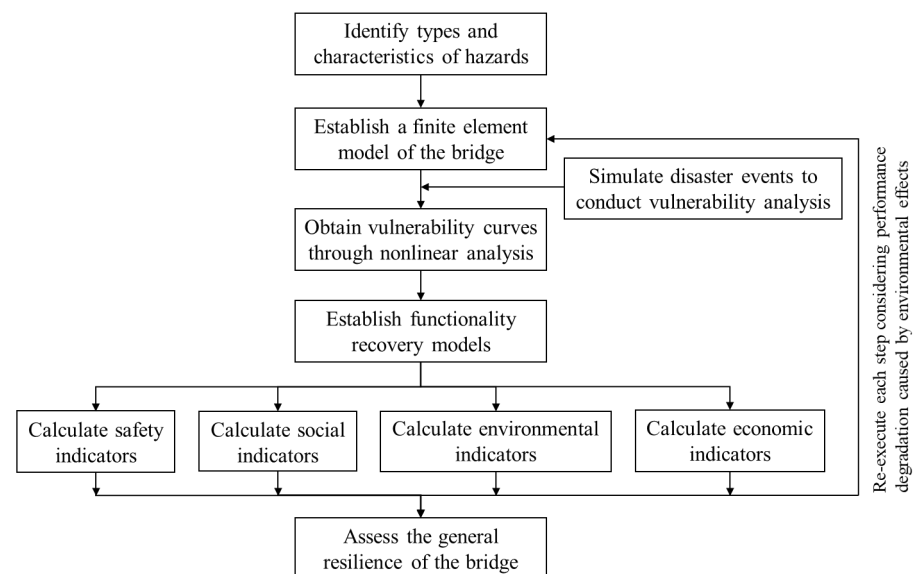


**Figure 4.** Bridge resilience assessment process.

Step 1 involves the identification of types and characteristics of hazards, which encompasses a clear definition of hazards in the environment where the bridge is located, which is accompanied by an analysis of potential hazard scenarios through probability-based hazard analysis.

Step 2 establishes a finite element model that accurately captures the bridge's characteristics. Then, a nonlinear analysis is conducted based on the hazards identified in Step 1, yielding vulnerability curves of the bridge for various damage states and the identification of vulnerable components.

In Step 3, a probabilistic analysis of failure is executed. The failure probability of the bridge in different damage states under specific hazard intensities is calculated utilizing the vulnerability curves derived in Step 2.

Step 4 focuses on the establishment of functionality recovery models. Diverse repair strategies are proposed, considering factors such as existing resources, practical requirements, hazard scenarios, and structural damage conditions.

Step 5 encompasses the evaluation of the generalized bridge resilience through the proposed four indicators. Furthermore, an analysis and comparison of different repair strategies are undertaken.

Finally, in Step 6, the structural performance degradation over the bridge's service life due to environmental factors is considered, involving updating the finite element model and reiterating Steps 2 to 5.

### 2.3. Multi-Dimensional Evaluation Indicators for Bridge Resilience

In order to combine safety, social, environmental, and economic impacts, the generalized bridge resilience is assessed using various resilience evaluation indicators in this study. The specific meanings of these multi-dimensional evaluation indicators, along with their corresponding determination methods, are explained in detail below.

#### 2.3.1. Safety Indicators

Safety indicators mainly focus on a bridge's structural integrity and the ability to resist disasters, involving analyzing vulnerability, estimating damage states, assessing residual capacity, and evaluating post-disaster recovery capacity, which can be determined through the following steps.

Firstly, the environment in which the bridge is located and the types and scenarios of disasters to which it may be subjected are clarified. Then, a vulnerability analysis of the bridge under disasters is conducted, considering factors such as the history of load effects and performance degradation, to obtain the failure probabilities under different damage states. Subsequently, a rational functionality recovery model is employed to simulate the post-disaster repair of the structure and construct bridge functionality curves for specific disaster scenarios. Lastly, the estimated structural resilience value calculated through Equation (4) is used as a safety indicator.

The calculation methods for the failure probabilities of bridge structures vary for different disasters. Currently, the vulnerability analysis method based on numerical simulation analysis is widely applied in the field of bridge disaster resistance [26–28], which will not be elaborated upon in this paper due to space limitations.

#### 2.3.2. Social Indicators

Social indicators aim to assess the impact of bridge failures on human life and social activities. Following a disaster event, it may be necessary to temporarily close a bridge to ensure the safety of both the structure and the individuals who use it. The length of this closure period can significantly impact the daily lives and productivity of those living in the vicinity of the bridge. Furthermore, in the case of severe disasters, a certain number of casualties may occur, leading to a profound societal impact. Therefore, this paper considers both the closure duration and the number of fatalities as indicators for assessing the generalized bridge resilience.

The closure duration of a bridge under the influence of a disaster event can be calculated by the following equation:

$$DT(t) = \sum_{i=1}^5 P_{DS_i|IM}(t) \cdot d_i \quad (5)$$

where  $d_i$  represents the downtime corresponding to different damage states.

Based on reference [29] and engineering experience, the estimated closure duration of bridges in various damage states is presented in Table 1.

**Table 1.** Estimated closure duration of bridges.

Damage State	No Damage	Slight Damage	Moderate Damage	Extensive Damage	Complete Damage
$d_i$ (day)	0	7	30	120	365

The number of fatalities following a disaster event is estimated with the following equation:

$$FA(t) = \sum_{i=1}^5 P_{DS_i|IM}(t) \cdot FT_i \quad (6)$$

where  $FT_i$  represents the average number of fatalities associated with a specific damage state, which can be obtained through the statistical analysis of the actual number of casualties following the occurrence of a hazard.

Combining reference [30] and engineering experience, the estimated number of fatalities for bridges in different damage states is presented in Table 2.

**Table 2.** Estimated number of fatalities.

Damage State	No Damage	Slight Damage	Moderate Damage	Extensive Damage	Complete Damage
$FT_i$	0	0.2	0.6	1.2	4.2

### 2.3.3. Environmental Indicators

Environmental indicators are used to evaluate the ecological consequences of bridge failures. In the entire lifecycle of a structure, resource conservation, environmental protection, pollution reduction, and achieving harmonious coexistence between human and nature are crucial aspects of future urban ecology. Therefore, it is imperative to take into account the environmental impact when assessing the generalized bridge resilience.

Carbon dioxide (CO<sub>2</sub>) stands as the primary greenhouse gas generated by human activities. After a disaster event, the closure of bridges compels a substantial number of vehicles to seek alternative routes. These detours typically require more time and cover longer distances, resulting in significant CO<sub>2</sub> emissions. Given that cars and trucks represent the primary vehicle types affected by bridge closures, environmental indicators can be obtained according to Equation (7).

$$EN(t) = \sum_{i=1}^5 P_{DS_i|IM}(t) A(t) D_i d_i \left[ E_{c,car} \left( 1 - \frac{T}{100} \right) + E_{c,truck} \frac{T}{100} \right] \quad (7)$$

where  $E_{c,car}$  and  $E_{c,truck}$  represent the CO<sub>2</sub> emissions per unit distance caused by cars and trucks.  $D_i$  is the detour distance.  $A(t)$  represents the average daily traffic for the structure's service life at time  $t$ , which is abbreviated as ADT.  $T$  denotes the proportion of trucks in the average daily traffic, which is abbreviated as ADTT.

Additionally, the process of structural restoration can also result in significant CO<sub>2</sub> emissions. For different structural damage states, the environmental impact of the structural repair can be estimated by multiplying the structural volume by the emission factor per unit volume [31].

### 2.3.4. Economic Indicators

Economic indicators serve as metrics to measure the financial implications of bridge failures. The repair of structural damage requires a certain amount of financial expenditure, and vehicle detours increase transportation costs. Consequently, the economic losses stemming from a disaster event can be classified into direct economic losses and indirect economic losses.



The direct economic losses, which include repair or reconstruction costs, the construction of temporary alternative structures, and debris removal and cleanup expenses, can be obtained according to Equation (8), assuming that these costs are proportional to the bridge's construction cost and that the proportionality coefficients depend on the bridge's damage state [32,33].

$$C_{REP,i} = WL \sum_{j=1}^{N_{out}} [P_{ij}(c_{reb}d_{r,j} + c_{rem})](1+r)^t \quad (8)$$

where  $W$  and  $L$  represent the width and length of the main beam.  $c_{reb}$  is the reconstruction cost per square meter.  $d_{r,j}$  is the damage ratio of the structure.  $c_{rem}$  is the cost of structure debris removal and site cleaning per square meter.  $P_{ij}$  is the failure probability in different damage states, and  $r$  is the currency discount rate.

Indirect economic losses are primarily caused by post-disaster traffic disruptions. The overall indirect economic loss consists of three components: vehicle operation costs, personnel and goods storage costs resulting from vehicle detours, and costs related to casualties.

Given the assumption that traffic flow distribution on the damaged bridge and detour routes was in equilibrium before the disaster, with the daily traffic volume depending on their respective carrying capacities, we can derive the total traffic flow by considering the traffic-carrying capacities of the damaged bridge ( $F_{c,l}$ ) and the detour route ( $F_{c,d}$ ). This can be expressed using the following equation:

$$A_{tot} = \frac{A_l(F_{c,l}n_{l,l} + F_{c,d}n_{l,d})}{F_{c,l}n_{l,l}} \quad (9)$$

where  $A_l$  and  $A_{tot}$  represent the traffic volumes on the damaged bridge and the total daily traffic volume.  $n_{l,l}$  and  $n_{l,d}$  denote the number of lanes on the damaged bridge and the detour route. Correspondingly, the daily traffic flow on the detour route ( $A_d$ ) is given below:

$$A_d = \frac{A_{tot}F_{c,d}n_{l,d}}{F_{c,l}n_{l,l} + F_{c,d}n_{l,d}} \quad (10)$$

The traffic flow on both the damaged bridge and the detour route experiences alterations, since the functionality of the structure undergoes changes over time. The variation in daily traffic volume can be determined based on the real-time functionality, as shown in Equation (11).

$$A'_{l,ij}(t) = \frac{A_{tot}F_{c,l}n_{l,l}Q_{ij}(t)}{F_{c,l}n_{l,l}Q_{ij}(t) + F_{c,d}n_{l,d}} A'_{d,ij}(t) = \frac{A_{tot}F_{c,d}n_{l,d}}{F_{c,l}n_{l,l}Q_{ij}(t) + F_{c,d}n_{l,d}} \quad (11)$$

where  $A'_{l,ij}(t)$  and  $A'_{d,ij}(t)$  represent the daily traffic volume at different time points on both the damaged bridge and the detour route following the occurrence of a disaster.

Following the occurrence of a disaster, vehicles are required to take detours, which typically involve longer travel distances than the pre-damage routes. This leads to increased time and energy consumption during travel, resulting in increased costs for both vehicle operation and manpower. Considering that the main types of vehicles on the bridge are cars and trucks, the cost of vehicle operation [33] is estimated using Equation (12).

$$C_{Run,i} = \sum_{j=1}^{N_{out}} \left\{ P_{ij} D_l [c_{run,car}(1-\tau) + c_{run,truck}\tau] \int_{t_0}^{t_h} [A'_{d,ij}(t) - A_d] dt \right\} \quad (12)$$

where  $c_{run,car}$  and  $c_{run,truck}$  represent the costs associated with driving cars and trucks, respectively.  $\tau$  represents the proportion of trucks in the daily traffic flow.  $D_l$  is the additional detour distance.  $t_0$  is the time of the disaster occurrence, and  $t_h$  is the period of functionality restoration.

The second indirect economic loss, i.e., the costs associated with the storage of personnel and goods resulting from vehicle detours [33], can be calculated with Equation (13):

$$C_{TL,i} = \left[ c_{AW} O_{car} \left( 1 - \frac{T}{100} \right) + \left( c_{ATC} O_{truck} + c_{goods} \right) \frac{T}{100} \right] \frac{D_I A(t) d_i}{S} \quad (13)$$

where  $c_{AW}$  represents the salary of car drivers,  $c_{ATC}$  represents the salary of truck drivers,  $c_{goods}$  represents the price of goods transportation,  $O_{car}$  and  $O_{truck}$  are the passenger capacities of cars and trucks, respectively.  $S$  is the average speed of vehicle detours.

For the last one, the loss of life resulting from different damage states [34] can be obtained with Equation (14).

$$C_{SL,i} = FT_i \cdot ICAF \quad (14)$$

where  $ICAF$  represents the implied cost of averting a fatality.

In summary, the formula for calculating the total indirect economic loss considering the discount rate  $r$  is as shown in Equation (15).

$$L_{ENC}(t) = \sum_{i=1}^5 P_{DS_i|IM}(t) (C_{Run,i} + C_{TL,i} + C_{SL,i}) (1+r)^t \quad (15)$$

### 3. Bridge Resilience Assessment under Vehicle-Induced Disaster: A Case Study

According to the bridge resilience assessment method proposed in Section 2, the resilience indicators can be calculated and assessed. Here, the resilience of bridges under vehicle-induced disaster scenarios is taken as an example to manifest the proposed method. Different repair strategies are compared to assist decision-makers in selecting appropriate repair approaches. Specifically, in this section, the resilience of a long-span cable-stayed bridge under a tanker truck explosion disaster is analyzed.

To analyze the vulnerability of the bridge under vehicle-induced blast, it is firstly required to have a clear understanding of the bridge's response and damage levels under different disaster scenarios. The overall layout of the cable-stayed bridge studied in this paper is illustrated in Figure 5, and the structural failure mode of the steel box girder under the explosive effect equivalent to 2500 kg TNT is depicted in Figure 6. Owing to space limitations, the intricacies of the investigation into explosion-related losses are not expounded upon here. The residual carrying capacity of steel box girders, selected as the parameter for damage degree classification, is determined through extensive finite element simulations capturing the nonlinear dynamic response and damage of bridges, and the vulnerability curve of bridges under vehicle-induced blast is illustrated in Figure 7. The vulnerability curve allows for the derivation of failure probabilities corresponding to different damage states of the bridge under varying disaster intensities and enables the commencement of resilience analysis.

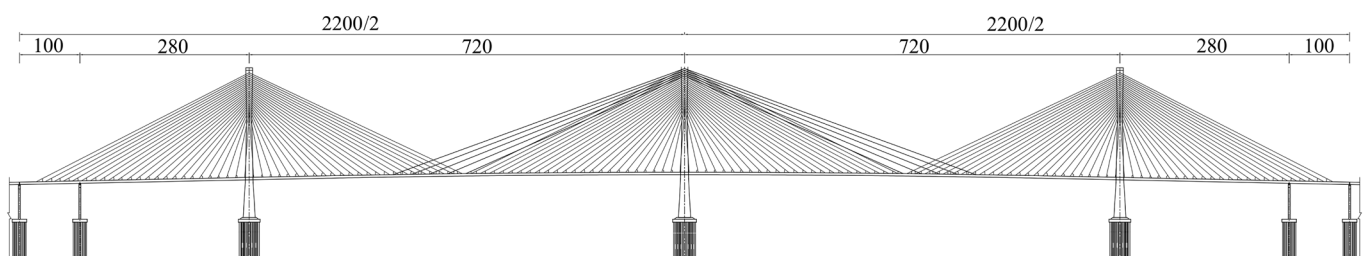


Figure 5. The overall layout of the cable-stayed bridge (unit: m).

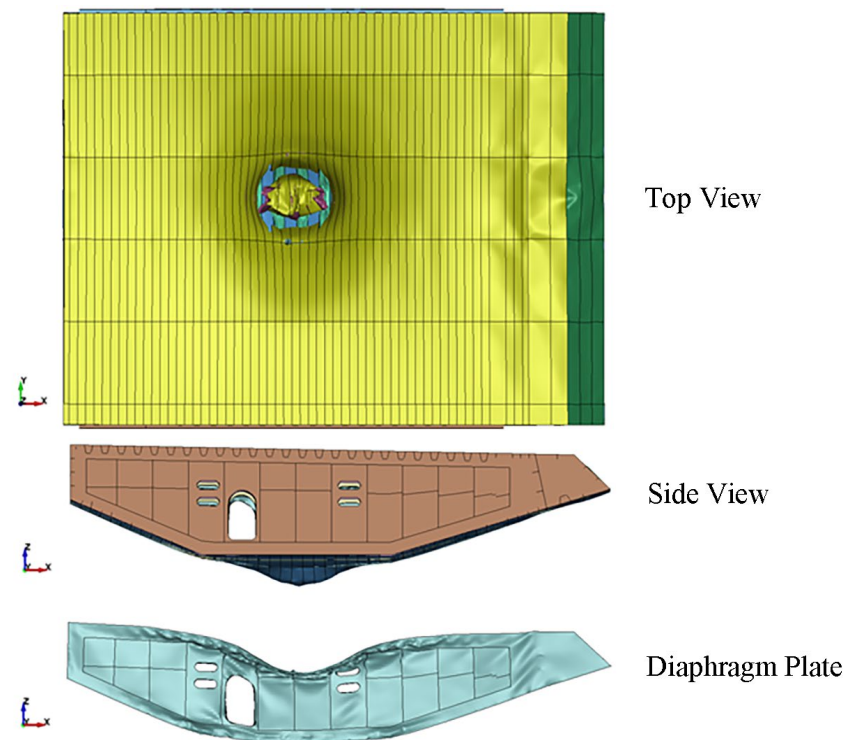


Figure 6. Structural failure mode of the steel box girder.

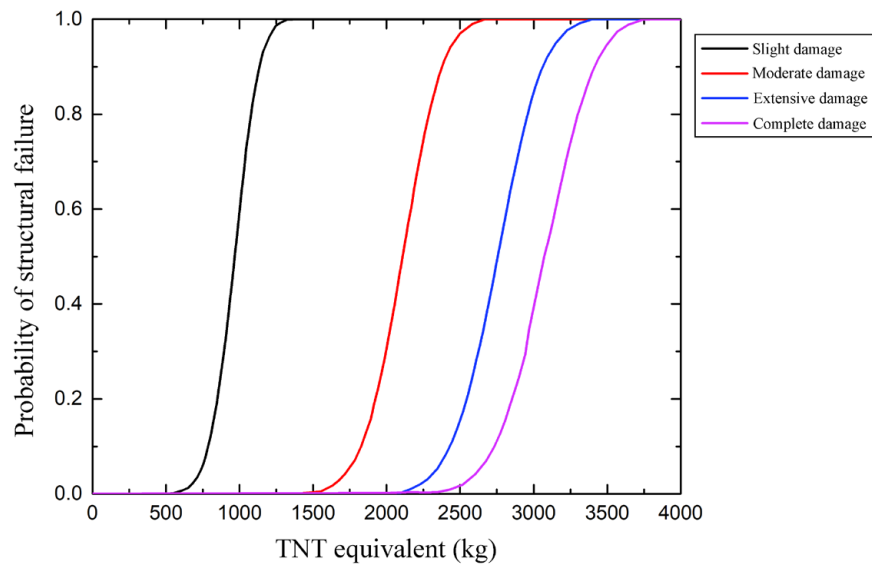


Figure 7. Vulnerability curve of bridges under vehicle-induced blast.

The values and distributions of the parameters for the bridge functionality recovery model under vehicle-induced blast [24,32,35] are given in Table 3. Specifically, for the parameters of residual functionality ( $Q_r$ ) and recovery duration ( $\delta_r$ ), their values are determined for undamaged and fully damaged states. For other damage states, these values follow a triangular distribution. Idle time  $\delta_i$  follows a uniform distribution, and the target functionality value and shape parameters have predetermined values.

**Table 3.** The values and distributions of parameters for the bridge functionality recovery model under explosive actions.

Parameters	Symbol	No Damage	Slight Damage	Moderate Damage	Extensive Damage	Complete Damage
Residual functionality	$Q_r$	1	min = 0.50 mode = 0.75 max = 1.00	min = 0.00 mode = 0.25 max = 0.50	min = 0.00 mode = 0.1 max = 0.2	0
Idle time (month)	$\delta_i$	/	min = 1 max = 2	min = 1 max = 2	min = 1 max = 2	min = 1 max = 2
Recovery Duration (month)	$\delta_r$	/	min = 1.50 mode = 3.00 max = 4.50	min = 4.00 mode = 6.00 max = 8.00	min = 6.00 mode = 8.00 max = 10.00	min = 6.00 mode = 8.00 max = 10.00
Target functionality	$Q_t$	/	1	1	1	1
Shape parameter	$s$ $A$	/ /	0.1 0	0.5 −0.1	0.9 0.1	0.9 0.1

The statistical characteristics of the parameters required for the generalized bridge resilience analysis are outlined in Table 4. These parameters are selected based on assumptions derived from engineering context and relevant research [30,31,34,36–40].

**Table 4.** Statistical characteristics of the parameters required for resilience analysis.

Parameters	Mean	Coefficient of Variation	Distribution Type	Source
ADT	29,500	0.2	Log-Normal	FHWA [36]
ADTT	0.13	0.2	Log-Normal	FHWA [36]
$D_l$ (km)	2.9	/	/	Decò et al. [37]
$F_{c,l}$ (vehicle/hour/lane)	2000	/	/	Assumed
$F_{c,d}$ (vehicle/hour/lane)	1000	/	/	Assumed
$n_{l,l}$	2	/	/	Assumed
$n_{l,d}$	1	/	/	Assumed
ICAF (\$)	160,000	/	/	Rackwitz [34]
$c_{run,car}$ (\$/km)	0.4	0.2	Log-Normal	AASHTO [38]
$c_{run,truck}$ (\$/km)	0.57	0.2	Log-Normal	AASHTO [38]
$c_{AW}$ (\$/h)	22.82	0.15	Log-Normal	Decò et al. [37]
$c_{ATC}$ (\$/h)	26.97	0.15	Log-Normal	Decò et al. [37]
$O_{car}$	1.5	0.15	Log-Normal	Decò et al. [37]
$O_{truck}$	1.05	0.15	Log-Normal	Decò et al. [37]
$c_{goods}$ (\$/h)	4	0.2	Log-Normal	Decò et al. [37]
$S$ (km/h)	50	0.15	Log-Normal	Decò et al. [37]
$E_{c,car}$ (kg/km)	0.22	0.2	Log-Normal	Gallivan et al. [30]
$E_{c,truck}$ (kg/km)	0.56	0.2	Log-Normal	Gallivan et al. [30]
$E_{c,concrete}$ (kg/m <sup>3</sup> )	376	0.2	Log-Normal	Tapia et al. [31]
$E_{c,steel}$ (kg/m <sup>3</sup> )	9749	0.2	Log-Normal	Tapia et al. [31]
Parameters	Minimum value	Maximum value	Distribution Type	Source
$c_{rem}$ (\$/m <sup>2</sup> )	224	560	Uniform	DOT-FL [39]
$c_{reb}$ (\$/m <sup>2</sup> )	1318	3294	Uniform	Caltrans [40]

### 3.1. Safety Indicators

The scenario involving a vehicle-induced blast with a 2500 kg equivalent TNT is taken as an analytical case, and the functionality recovery curve of the bridge is depicted in Figure 8. Without taking the degradation of bridge structural performance due to environmental factors into account, it is assumed that the initial functionality value of the bridge is 1 when the disaster occurred. The structural resilience value calculated through Equation (4) is 0.816.

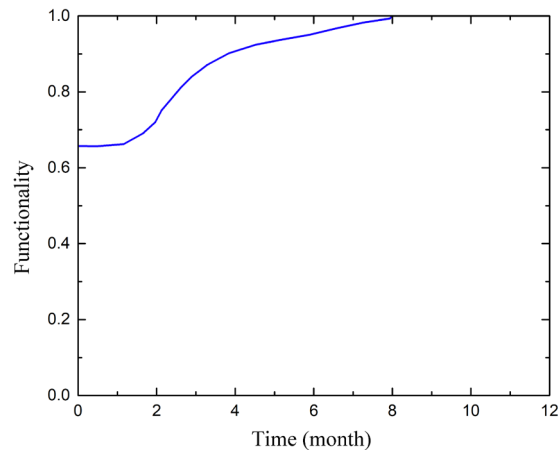


**Figure 8.** Functionality recovery curve of bridge under vehicle-induced blast.

In this study, the impact of structural performance degradation caused by chloride ion corrosion is considered using a uniform corrosion model. But the specific finite element simulation and calculation process of chloride diffusion, reinforcement corrosion, concrete carbonation, and bridge structural performance degradation will not be developed in this paper because of space limitations.

The impact of environmental effects on structural functionality is minimal during the initial 10 years, as indicated by the calculation results. However, as the bridge ages, the performance degradation caused by environmental influences leads to a gradual decline in bridge functionality. Upon integrating the degradation of bridge functionality caused by environmental effects into the calculation, the safety indicator of the bridge resilience, as a function of the bridge's age at the time of the disaster, is depicted in Figure 9. The trend of the curve underscores the importance of considering environmental effects in assessing bridge resilience and highlights the need for timely repairs and maintenance to mitigate the impact of aging and degradation on safety.

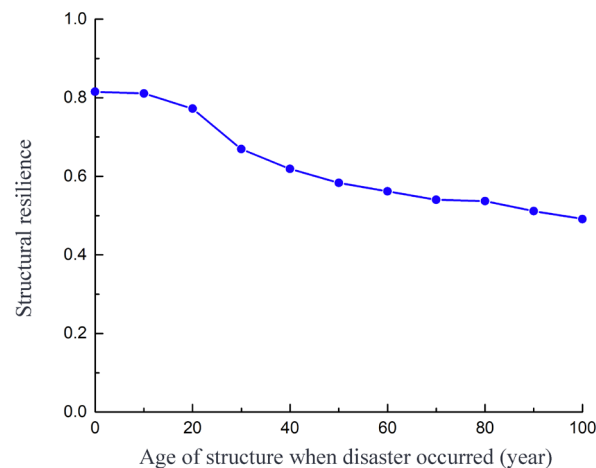


**Figure 9.** Bridge resilience safety indicator under vehicle-induced blast.

### 3.2. Social Indicators

The social indicators of bridge resilience include the duration of bridge closure and the number of fatalities, as determined by Equations (5) and (6) given in Section 2.3.2. In this section, the estimated values for bridge closure durations corresponding to different damage states are referenced from Table 1, and the estimates for the number of fatalities are derived from Table 2. These enable us to illustrate the variations in bridge closure duration and the number of fatalities resulting from vehicle-induced blast scenarios as a function of the age of the bridge structure because of environmental influences, as depicted in Figure 10.

It is evident that as the structural performance deteriorates over time, the social indicators, namely, bridge closure duration and the number of fatalities, continuously increase.

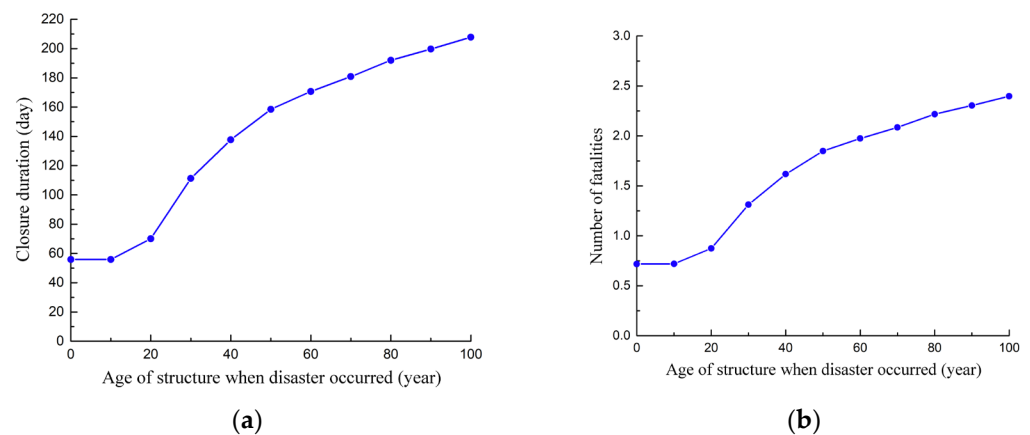


**Figure 10.** Bridge resilience social indicator under vehicle-induced blast. (a) Closure duration; (b) number of fatalities.

### 3.3. Environmental Indicators

The environmental indicators of bridge resilience are closely tied to the post-disaster functionality restoration process. The variation in the monthly average number of detoured vehicles during the functionality restoration process for bridges with different ages is depicted in Figure 11. As observed from the graph, as the bridge ages, the continuous degradation of structural performance leads to a decrease in safety and an increased probability of experiencing higher-level damage, culminating in diminished post-disaster functionality. Consequently, the number of vehicles necessitating detours within the bridge's associated transportation network rises.

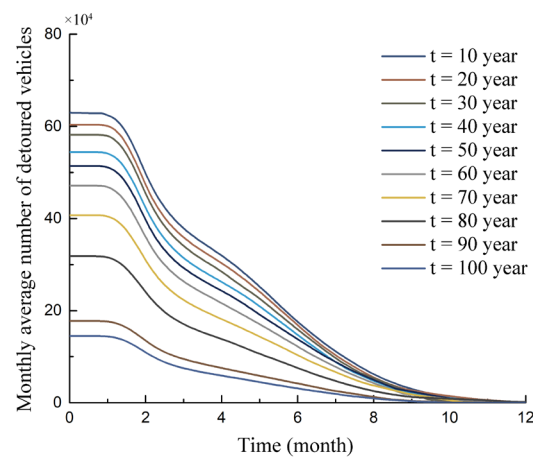


**Figure 11.** Monthly average number of detoured vehicles.

As manifested in Section 2.3.3, the  $\text{CO}_2$  emissions generated by vehicle detours can be obtained by employing Equation (7), and those stemming from structural repair or reconstruction can be calculated as a weighted sum of the impacts for different damage states, which is weighted by their failure probabilities. Referring to the statistical characteristics and values provided in Table 4, the changes in  $\text{CO}_2$  emissions for the bridge over its years of service are depicted in Figure 12. It can be observed that with the increase in the bridge's age, the demands for repair or reconstruction grow, resulting in more vehicle detours and a continuous rise in  $\text{CO}_2$  emissions. Therefore, to build a sustainable, environmentally friendly structure ecosystem, it is essential to consider not only safety and economic aspects but also potential environmental impacts.

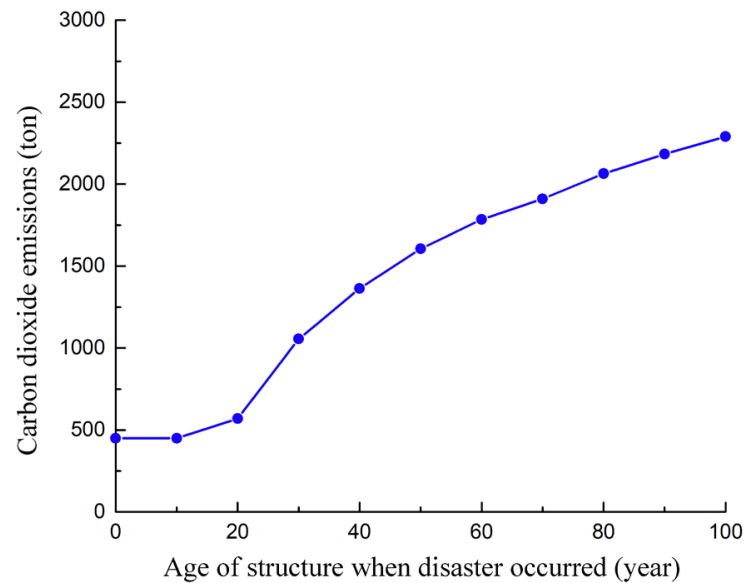


**Figure 12.** Bridge resilience environmental indicator under vehicle-induced blast.

### 3.4. Economic Indicators

Based on the statistical characteristics and values provided in Table 4, assuming an annual discount rate of 2%, the total economic losses are calculated through Equation (15). The changes in economic losses for different categories with respect to the age of bridge under blast scenarios are illustrated in Figures 13 and 14. It is evident from the figures that among all categories of economic losses, the expenses related to vehicle detours are the highest, followed by the costs of structural reconstruction and repair, and the losses due to casualties, while expenses for structural debris removal and site clearance are the lowest. Direct economic losses are significantly smaller than indirect economic losses, and all categories of economic losses increase noticeably with the growth of bridge's age. Therefore, in such disaster scenarios, indirect losses constitute the majority of total economic losses, while the expenses related to structural repair and reconstruction are relatively low. This provides us some inspiration: implementing rational repair strategies while focusing on controlling indirect losses due to vehicle detours can effectively reduce the overall economic expenditure during disaster events. This approach can lead to better long-term benefits for the structure.

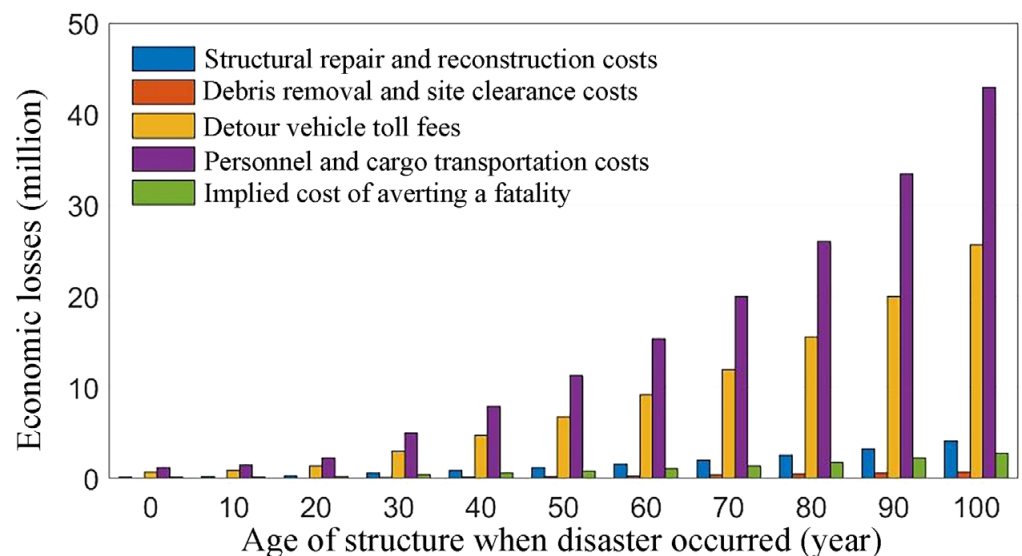


**Figure 13.** Economic losses for different categories.

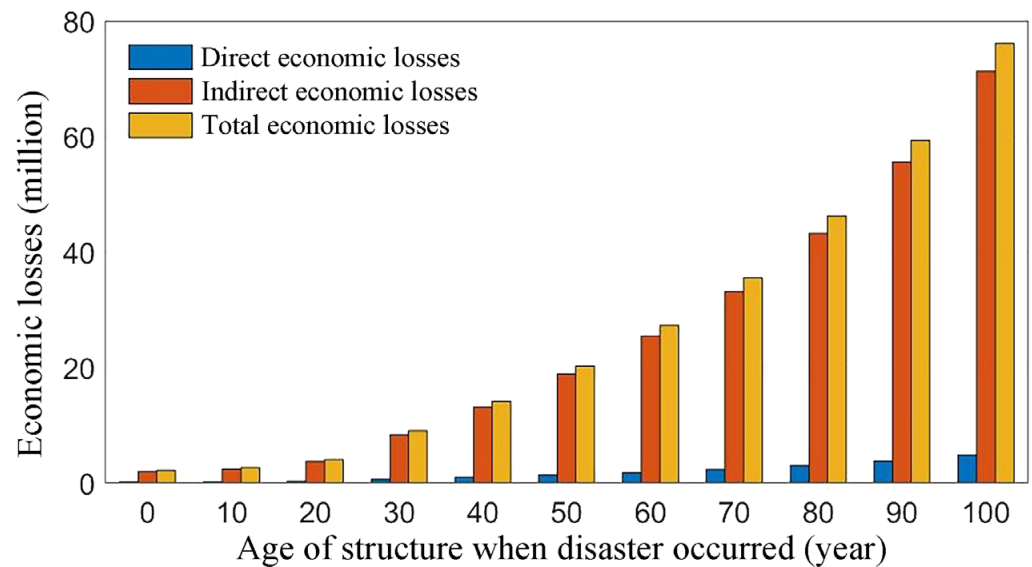


Figure 14. Bridge resilience economic indicator under vehicle-induced blast.

#### 4. Bridge Repair Decision Making under Vehicle-Induced Disaster

After a disaster, various repair strategies can be employed to restore a bridge, and the choice of repair strategy directly impacts the generalized resilience assessment of the bridge. Therefore, with the aim of providing guidance for decision making in bridge disaster recovery, this study explores possible repair strategies considering the influence of repair speed. Different recovery speeds have a direct impact on the duration and economic expenses of the repair process. Generally, structural repair can be carried out at three different speeds: fast, normal, and slow. By considering the influence of recovery speed through different values of correction coefficients [41], correction coefficients for repair time  $V_t$  and economic losses  $V_c$  are introduced. Here,  $V_t$  takes values of  $\pm 20\%$ , and  $V_c$  takes values of  $\pm 15\%$ .

For each damage state of the bridge, multiple repair methods can be chosen. The combination of different repair methods for various damage states forms a complete set of repair strategies, as shown in Table 5. For example, without considering budget constraints, Strategy 3 indicates that for slight, moderate, extensive, and complete damage states, the fastest recovery speed is applied to restore the functionality to its original state in the shortest possible time.

Table 5. Repair strategies considering the impact of recovery speed.

Strategy Number	Restoration Speed under Different Damage States			
	Slight Damage	Moderate Damage	Extensive Damage	Complete Damage
1	Slow	Slow	Slow	Slow
2	Normal	Normal	Normal	Normal
3	Fast	Fast	Fast	Fast
4	No repair	No repair	No repair	No repair
5	No repair	No repair	Slow	Slow
6	No repair	No repair	Normal	Normal
7	No repair	No repair	Fast	Fast
8	Slow	Slow	No repair	No repair
9	Normal	Normal	No repair	No repair
10	Fast	Fast	No repair	No repair
11	Slow	Slow	Normal	Normal
12	Normal	Normal	Fast	Fast
13	Normal	Normal	Slow	Slow
14	Fast	Fast	Normal	Normal



#### 4.1. Safety Indicators and Recovery Speed under Varied Repair Strategies

Based on the statistical characteristics and parameter values of bridge recovery models, the following scenario are taken as an example: the functional recovery target value is 100%, the relevant time range for structural elasticity is 15 months after the disaster, and the calculation time interval is 1/100 of a month. Subsequently, using the repair strategies provided in Table 5 and the Monte Carlo random sampling method, 5000 samples are extracted to obtain the parameters of the functional recovery model for each damage state. Next, the sampling results for different damage states are weighted based on their corresponding structural failure probabilities, thus combining them together. Finally, the functional recovery curves for the 14 strategies are estimated using mean estimation. According to the definitions of structural resilience and functionality restoration speed, the mean and standard deviation of functionality restoration samples for different strategies are calculated.

The calculation results are depicted in Figures 15 and 16, where the height of the bars represents the mean values, and the black dashed lines indicate plus or minus one standard deviation. From these figures, it can be observed that the structural resilience variation is relatively small among different repair strategies, while the repair speed exhibits greater variation. Strategy 3, involving fast repairs for all damage states, shows the maximum structural resilience and the fastest repair speed. On the other hand, Strategy 4, which involves no repair measures for any damage state, corresponds to the minimum structural resilience with a repair speed of 0. Strategies 5–10 exhibit relatively lower structural resilience and repair rates due to the presence of unrepaired damage states. However, for Strategies 4–7, the standard deviation of structural resilience is comparatively large. Strategies with higher structural resilience tend to have smaller standard deviations.

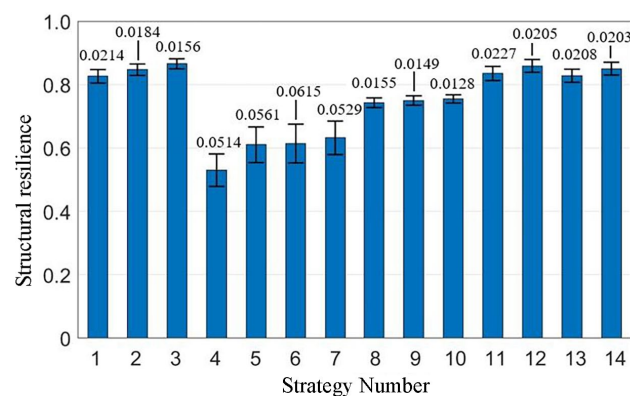


Figure 15. Safety indicators under different repair strategies.

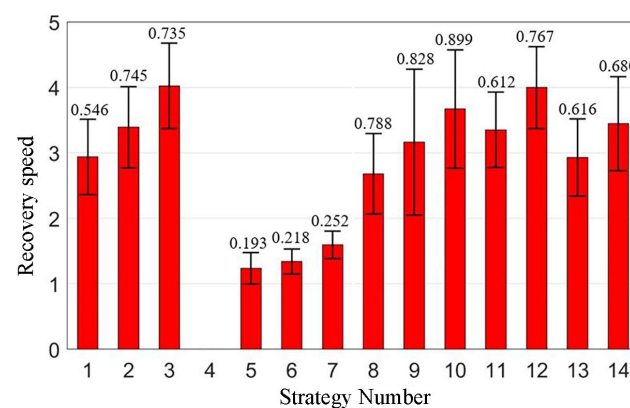


Figure 16. Recovery speed under different repair strategies.

#### 4.2. Impact of Different Repair Strategies on Social Indicators

Under the impact of disasters, the societal indicators of the generalized resilience of bridges include post-disaster downtime and the number of casualties. Since the number of casualties is directly related to the extent of structural damage under disaster conditions and is unrelated to subsequent repair efforts, the influence of repair strategies on this indicator is not considered. Assuming that structural functional restoration commences immediately after the occurrence of a disaster, and the bridge is opened for traffic immediately upon completion of the restoration, the downtime corresponds to the duration of structural functional recovery. Considering the relationship between the recovery speed of the structure and the recovery time, Figure 16 also reflects the varying durations of bridge recovery time associated with different repair strategies.

#### 4.3. Environmental Indicators under Varied Repair Strategies

The CO<sub>2</sub> emissions resulting from different repair strategies are illustrated in Figure 17. As depicted in the graph, the carbon emissions from vehicle detours are approximately 100 times higher than the associated values for structural repair. Comparing Strategies 1–3 and 5–7 highlights that faster repair speeds and concentrated resource allocation result in higher carbon emissions during structural restoration with vehicle detour emissions comparatively smaller.

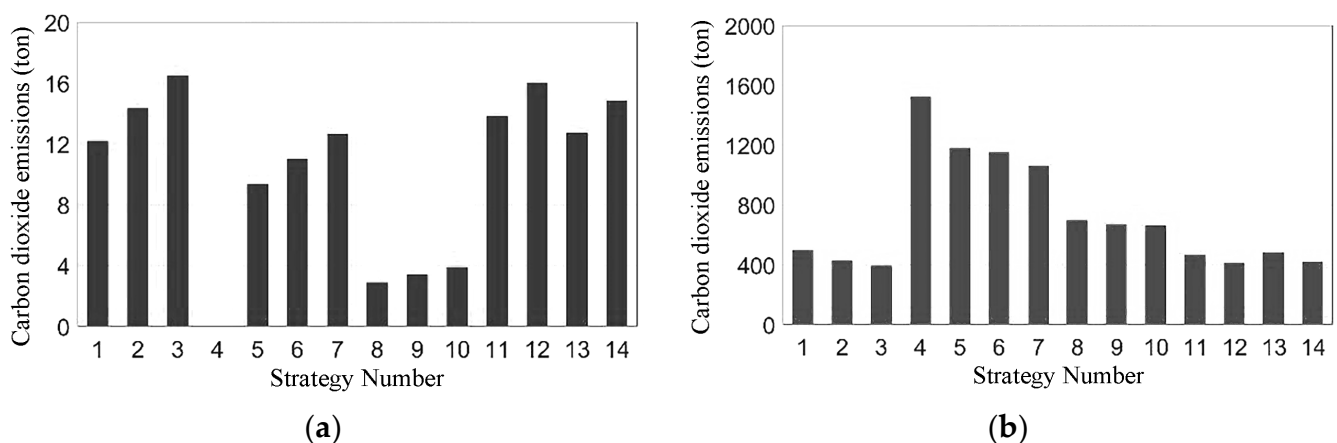


**Figure 17.** The environmental impacts associated with different repair strategies. (a) CO<sub>2</sub> emissions from structural rehabilitation; (b) CO<sub>2</sub> emissions from vehicle detours.

#### 4.4. Impact of Different Repair Strategies on Economic Indicators

According to the definition of the economic indicators, diverse economic expenditures associated with distinct repair strategies are calculated, as shown in Figure 18. A comparative analysis of Strategies 1–3 and 5–7 reveals that heightened recovery speed correlates with diminished time for complete restoration, augmented structural resilience, and an escalation in direct economic investment. Concurrently, indirect economic losses exhibit a reduction. Irrespective of the chosen strategy, indirect economic losses consistently represent the predominant share within various expenditure categories. Consequently, judicious investment in structural construction and repair processes can effectively mitigate post-disaster indirect economic losses, thereby diminishing overall economic losses and enhancing economic efficiency across the entire structural lifecycle.

The relationship between structural resilience, direct economic losses, and the environmental indicator under different repair strategies after a vehicle-induced blast is illustrated in Figures 19 and 20. The order of strategies in the figures is arranged in descending order based on the estimated values of structural resilience. From the graphs, it is evident that if the owner and professional technical personnel aim to achieve the fastest restoration to reduce economic losses during the recovery process, Strategy 3, despite its substantial direct economic investment, minimizes indirect economic losses to the lowest extent, which

corresponds to the highest structural resilience and minimal environmental impact, making it the optimal choice in this scenario.

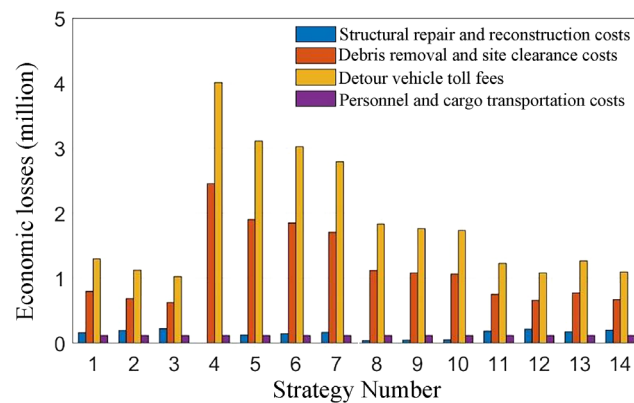


Figure 18. Economic losses under different repair strategies.

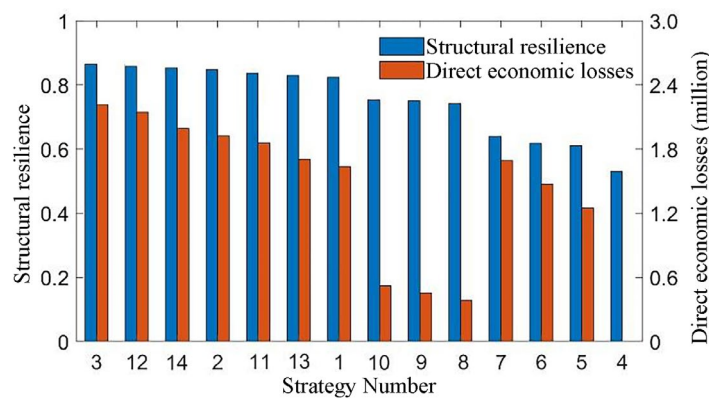


Figure 19. Structural resilience and direct economic losses under different repair strategies.

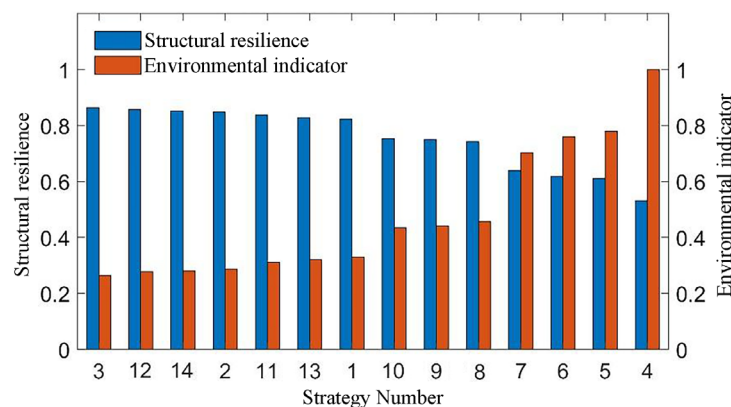


Figure 20. Structural resilience and comprehensive environmental impact under different repair strategies.

In summary, conducting a generalized resilience assessment for bridges under the impact of disasters, calculating safety, societal, environmental, and economic four-dimensional evaluation indicators, and comparing different repair strategies can assist owners or professional technical personnel in making informed decisions. The selection of an appropriate repair strategy for functionality restoration can be based on various engineering requirements and deployable resources.

## 5. Conclusions

This study proposes the concept of generalized bridge resilience and presents a multi-dimensional indicator system encompassing safety, society, environment, and economy. A method for assessment of generalized resilience is also introduced, enabling the management of disaster risk and cost throughout the lifecycle. An example of a large-span cable-stayed bridge under the impact of vehicle-induced blast is provided to manifest the proposed method, and the influence of repair speed and different repair strategies are illustrated in detail. A repair strategy analysis and comparison are conducted based on actual engineering requirements and deployable resources, providing decision-making recommendations. The main research conclusions are as follows:

- (1) Prior bridge resilience studies mainly focused on structural safety, overlooking the broader impact of disasters on society, the environment, and the regional economy. This study introduces the concept of generalized bridge resilience, which offers a comprehensive evaluation for disaster risk prediction and management across the entire bridge lifecycle, dynamically controlling resilience to enhance safety, economic efficiency, and environmentally friendly structural ecologies.
- (2) In the early stages, environmental factors minimally affect the functionality and resilience of bridge structures under disasters. However, with increasing bridge age, structural resistance, functionality, and disaster resilience decline. The time-dependent resilience of bridge structures, influenced by environmental factors causing performance degradation, requires consideration in resilience assessments throughout the lifecycle.
- (3) Indirect economic losses constitute the largest proportion among various economic expenditures. Adequate investment in structural restoration can effectively reduce indirect economic losses, particularly the time value of labor and goods due to vehicle detours, thereby reducing overall economic losses and enhancing the economic efficiency of the structure's entire lifecycle.
- (4) Significant direct economic investment can expedite functionality restoration, thereby effectively reducing indirect economic losses. Emphasizing strategies with enhanced structural resilience, shorter restoration times, and minimal environmental impact should be the priority while still meeting budget requirements. In the case studied in this research, Strategy 3 emerges as the optimal choice, which is characterized by minimal environmental impact, the highest structural resilience, and relatively low overall economic expenditure.

The specific data for the resilience analysis indicators proposed in this study are primarily applicable to the resilience assessment of long-span cable-stayed bridges under vehicle-induced blast. But the resilience evaluation method proposed in this study is not only applicable to vehicle-induced disasters and bridge structures but is also suitable for various other types of disasters and structural forms, demonstrating broad application prospects.

While this study has provided initial findings, there is a need for further research. Due to a lack of actual bridge repair data, the functionality recovery model proposed for bridges relies on engineering experience and existing literature, introducing some subjective limitations. Future research should involve on-site investigations of real disasters, the identification of potential functionality restoration measures, the validation of time and cost estimates for various repair measures, and the development of more accurate post-disaster functionality recovery models.

**Author Contributions:** Conceptualization, Y.L.; methodology, C.X. and Y.L.; formal analysis, Y.L.; data curation, Y.L.; writing—original draft preparation, Y.L.; writing—review and editing, C.X. All authors have read and agreed to the published version of the manuscript.

**Funding:** This research received no external funding.

**Institutional Review Board Statement:** Not applicable.

**Informed Consent Statement:** Not applicable.

**Data Availability Statement:** The data presented in this study are available on request from the corresponding author. The data are not publicly available due to privacy.

**Conflicts of Interest:** The authors declare no conflicts of interest.

## References

- Holling, C.S. Resilience and stability of ecological systems. *Annu. Rev. Ecol. Syst.* **1973**, *4*, 1–23. [[CrossRef](#)]
- Timmermann, P. Vulnerability, resilience and the collapse of society. *Environ. Monogr.* **1981**, *1*, 1–42.
- Bruneau, M.; Chang, S.E.; Eguchi, R.T.; Lee, G.C.; O'Rourke, T.D.; Reinhorn, A.M.; Shinozuka, M.; Tierney, K.; Wallace, W.A.; Von Winterfeldt, D. A framework to quantitatively assess and enhance the seismic resilience of communities. *Earthq. Spectra* **2003**, *19*, 733–752. [[CrossRef](#)]
- Rose, A. Defining and measuring economic resilience to disasters. *Disaster Prev. Manag.* **2004**, *13*, 307–314. [[CrossRef](#)]
- Miles, S.B.; Chang, S.E. Modeling community recovery from earthquakes. *Earthq. Spectra* **2006**, *22*, 439–458. [[CrossRef](#)]
- Coppola, D.P. *Introduction to International Disaster Management*; Butterworth Heinemann: Oxford, UK, 2007.
- Deptuła, A.M.; Stosiak, M.; Deptuła, A.; Lubecki, M.; Karpenko, M.; Skačkauskas, P.; Urbanowicz, K.; Danilevičius, A. Risk Assessment of Innovation Prototype for the Example Hydraulic Cylinder. *Sustainability* **2023**, *15*, 440. [[CrossRef](#)]
- Frangopol, D.M.; Bocchini, P. Bridge network performance, maintenance and optimisation under uncertainty: Accomplishments and challenges. In *Structures and Infrastructure Systems*; Routledge: London, UK, 2019; pp. 30–45.
- Cimellaro, G.P.; Reinhorn, A.M.; Bruneau, M. Framework for analytical quantification of disaster resilience. *Eng. Struct.* **2010**, *32*, 3639–3649. [[CrossRef](#)]
- Chang, S.E.; Shinozuka, M. Measuring improvements in the disaster resilience of communities. *Earthq. Spectra* **2004**, *20*, 739–755. [[CrossRef](#)]
- Martin, R.; Sunley, P. On the notion of regional economic resilience: Conceptualization and explanation. *J. Econ. Geogr.* **2015**, *15*, 1–42. [[CrossRef](#)]
- Zeng, X.; Yu, Y.; Yang, S.; Lv, Y.; Sarker, M.N.I. Urban resilience for urban sustainability: Concepts, dimensions, and perspectives. *Sustainability* **2022**, *14*, 2481. [[CrossRef](#)]
- Zhou, L.; Chen, Z. Measuring the Performance of Airport Resilience to Severe Weather Events. *Transp. Res. Part. D Transp. Environ.* **2020**, *83*, 102362. [[CrossRef](#)]
- Wei, D.; Chen, Z.; Rose, A. Evaluating the role of resilience in reducing economic losses from disasters: A multi-regional analysis of a seaport disruption. *Reg. Sci. Assoc. Int.* **2020**, *99*, 1691–1722. [[CrossRef](#)]
- Venkittaraman, A.; Banerjee, S. Enhancing resilience of highway bridges through seismic retrofit. *Earthq. Eng. Struct. Dyn.* **2014**, *43*, 1173–1191. [[CrossRef](#)]
- Alipour, A.; Shafei, B. Seismic resilience of transportation networks with deteriorating components. *J. Struct. Eng.* **2016**, *142*, C4015015. [[CrossRef](#)]
- Giouvanidis, A.I.; Dong, Y. Seismic loss and resilience assessment of single-column rocking bridges. *Bull. Earthq. Eng.* **2020**, *18*, 4481–4513. [[CrossRef](#)]
- Shen, Y.; Freddi, F.; Li, Y.; Li, J. Enhanced strategies for seismic resilient posttensioned reinforced concrete bridge piers: Experimental tests and numerical simulations. *J. Struct. Eng.* **2023**, *149*, 04022259. [[CrossRef](#)]
- Khan, S.A.; Kabir, G.; Billah, M.; Dutta, S. An integrated framework for bridge infrastructure resilience analysis against seismic hazard. *Sustain. Resilient Infrastruct.* **2023**, *8* (Suppl. 1), 5–25. [[CrossRef](#)]
- Cimellaro, G.P.; Reinhorn, A.M.; Bruneau, M. Seismic resilience of a hospital system. *Struct. Infrastruct. Eng.* **2010**, *6*, 127–144. [[CrossRef](#)]
- Bocchini, P.; Frangopol, D.M. Optimal resilience-and cost-based postdisaster intervention prioritization for bridges along a highway segment. *J. Bridge Eng.* **2012**, *17*, 117–129. [[CrossRef](#)]
- Kafali, C.; Grigoriu, M. Rehabilitation decision analysis. In Proceedings of the Ninth International Conference on Structural Safety and Reliability, Amsterdam, The Netherlands, 19–23 June 2005.
- Padgett, J.E.; DesRoches, R. Bridge functionality relationships for improved seismic risk assessment of transportation networks. *Earthq. Spectra* **2007**, *23*, 115–130. [[CrossRef](#)]
- Bocchini, P.; Decò, A.; Frangopol, D.M. Probabilistic functionality recovery model for resilience analysis. *Bridge Maint. Saf. Manag. Resil. Sustain.* **2012**, 1920–1927.
- Frangopol, D.M.; Bocchini, P. Resilience as optimization criterion for the rehabilitation of bridges belonging to a transportation network subject to earthquake. In Proceedings of the Structures Congress, Las Vegas, NV, USA, 14–16 April 2011.
- Hwang, H.; Jernigan, J.B.; Lin, Y.W. Evaluation of seismic damage to Memphis bridges and highway systems. *J. Bridge Eng.* **2000**, *5*, 322–330. [[CrossRef](#)]
- Karim, K.R.; Yamazaki, F. A simplified method of constructing fragility curves for highway bridges. *Earthq. Eng. Struct. Dyn.* **2003**, *32*, 1603–1626. [[CrossRef](#)]
- Mackie, K.R.; Stojadinović, B. Post-earthquake functionality of highway overpass bridges. *Earthq. Eng. Struct. Dyn.* **2006**, *35*, 77–93. [[CrossRef](#)]

29. Padgett, J.E.; Ghosh, J.; Dennemann, K. Sustainable infrastructure subjected to multiple threats. In *TCLÉE 2009: Lifeline Earthquake Engineering in a Multihazard Environment*; American Society of Civil Engineers: Reston, VA, USA, 2009; pp. 1–11.
30. Gallivan, F.; Ang-Olson, J.; Papsen, A. Greenhouse gas mitigation measures for transportation construction, maintenance, and operations activities. In Proceedings of the AASHTO Standing Committee on the Environment, San Francisco, CA, USA, April 2010.
31. Tapia, C.; Ghosh, J.; Padgett, J.E. Life cycle performance metrics for aging and seismically vulnerable bridges. In Proceedings of the Structures Congress, Las Vegas, NV, USA, 14–16 April 2011; pp. 1937–1948.
32. Shinozuka, M.; Zhou, Y.; Kim, S.; Murachi, Y.; Banerjee, S.; Cho, S.; Chung, H. *Socio-Economic Effect of Seismic Retrofit Implemented on Bridges in the Los Angeles Highway Network*; Department of Transportation: Sacramento, CA, USA, 2008.
33. Stein, S.M.; Young, G.K.; Trent, R.E.; Pearson, D.R. Prioritizing scour vulnerable bridges using risk. *J. Infrastruct. Syst.* **1999**, *5*, 95–101. [[CrossRef](#)]
34. Rackwitz, R. Optimization and risk acceptability based on the life quality index. *Struct. Saf.* **2002**, *24*, 297–331. [[CrossRef](#)]
35. Argyroudis, S.A.; Mitoulis, S.A.; Hofer, L.; Zanini, M.A.; Tubaldi, E.; Frangopol, D.M. Resilience assessment framework for critical infrastructure in a multi-hazard environment: Case study on transport assets. *Sci. Total Environ.* **2020**, *714*, 136854. [[CrossRef](#)] [[PubMed](#)]
36. FHWA. *National Bridge Inventory (NBI) Database*; U.S. Department of Transportation, Federal Highway Administration (FHWA): Washington, DC, UAS, 2010.
37. Decò, A.; Frangopol, D.M. Risk assessment of highway bridges under multiple hazards. *J. Risk Res.* **2011**, *14*, 1057–1089. [[CrossRef](#)]
38. AASHTO. *A Manual of User Benefit Analysis for Highways*, 2nd ed.; American Association of State Highway and Transportation Officials (AASHTO): Washington, DC, USA, 2003.
39. DOT-FL. *Transportation Costs Report*; State of Florida-Department of Transportation: Tallahassee, FL, USA, 2009.
40. Caltrans. *Comparative Bridge Costs*; California Department of Transportation: Sacramento, CA, USA, 2010.
41. Engius. *Case Study: Interstate 40 Bridge Reconstruction*; Engius: Webbers Falls, Oklahoma, 2002.

**Disclaimer/Publisher’s Note:** The statements, opinions and data contained in all publications are solely those of the individual author(s) and contributor(s) and not of MDPI and/or the editor(s). MDPI and/or the editor(s) disclaim responsibility for any injury to people or property resulting from any ideas, methods, instructions or products referred to in the content.